*Plasma Medicine*, 6(2): 125–134 (2016)

# Plasma-Tissue Interactions in Argon Plasma Coagulation: Effects of Power and Tissue Resistance

Eda Gjika,[a] David Scott,[a] Alexey Shashurin,[b] Taisen Zhuang,[c] Jerome Canady,[d] & Michael Keidar[a,*]

[a]Department of Mechanical and Aerospace Engineering, School of Engineering and Applied Science, George Washington University, Washington, DC, USA; [b]School of Aeronautics and Astronautics, Purdue University, West Lafayette, IN, USA; [c]US Medical Innovations (USMI), LLC Corporate Headquarters, Takoma Park, MD, USA; [d]Jerome Canady Research Institute for Advanced Biological and Technological Sciences, Takoma Park, MD, USA

*Address all correspondence to: Michael Keidar, Department of Mechanical and Aerospace Engineering, School of Engineering and Applied Science, George Washington University, Washington, DC, 20052, USA, E-mail: keidar@gwu.edu

**ABSTRACT:** The coagulation properties of the argon plasma coagulation (APC) technique present tremendous potential for a wide range of endoscopic applications. Although several studies have explored the endoscopic application of this technique, there has been no previous research about the relevant argon plasma properties during coagulation. We have investigated the role of power in the interactions between plasma and biological tissue, and have reported on the dielectric properties of the APC treated samples. The data revealed that at a resistance of 1 kΩ, the applied power was within 10% to 15% of the power setting, and the average resistance of the animal samples was between 0.8 and 3.7 kΩ. The data also suggested that the amount of power applied could be adjusted according to the expected tissue resistance range. Additionally, it was determined that the burned surface caused by the APC treatment was on average two to three times less conductive than the untreated surface. The data also revealed that 60%–80% of the power produced by the electrosurgical generator was delivered into the biological tissue, and the plasma channel consumed the remaining 20%–40%. This study establishes a guide for the investigation of optimal argon thermal plasma properties for biological tissue application.

**KEY WORDS:** power distribution, equivalent tissue resistance, tissue conductivity

## I. INTRODUCTION

Argon plasma coagulation (APC) was first used in surgery in the late 1970s and has since become one of the most common techniques utilized in electrosurgery. APC offers many potential applications, including tumor debulking, ablation of vascular malformations, and coagulation of peptic ulcer bleeding sites.[1–5] Common gastrointestinal (GI) diseases treated by APC include radiation proctitis, Barrett's esophagus, and gastric antral vascular ectasia (GAVE).[6–13]

APC is a preferable treatment method because it conducts electrical current without direct contact. The ability to ablate tissue without direct contact is beneficial, as it may

1947-5764/16/$35.00  

mitigate the risk of bleeding at the targeted site and the surrounding tissue. The scalpel is positioned 2–6 mm from the treatment site, and thermal heating is achieved by high purity ionized argon gas. The produced heat denatures the proteins and evaporates the intracellular and extracellular water, resulting in tissue destruction and coagulation.[2,3,6]

The tissue's response to thermal heating is directly dependent on the amount of power applied. The applied power ranges from 20 to 90 W based on the type of treatment.[14–17]

Although the applied power used for treatment is under investigation, little is known about the physical properties of plasma employed and the plasma-tissue interaction during coagulation. Basic plasma parameters, such as argon plasma density and electrical conductivity using Rayleigh microwave scattering, have been previously reported by our group.[28] Plasma density was determined to be in the range of $7.5–9.5 \times 10^{15}$ $cm^{-3}$, and the electrical conductivity was 1–2 $\Omega^{-1}cm^{-1}$.

In this paper we present data of plasma-tissue interactions during APC treatment, which was obtained by determining the accuracy of the power produced by the electrosurgical unit based on tissue resistance. To our knowledge, these plasma-tissue interactions have never been investigated before. We also elucidate the power distribution between plasma and tissue, and report on the conductivity of APC treated samples. A better understanding of these interactions would offer more insight into the properties of argon plasma and the amount of power required for an effective treatment.

## II. EXPERIMENTAL PARAMETERS

The experiments were conducted using the electrosurgical system SS-200E/Argon 2 (ESU) in combination with the electrosurgical scalpel by US Medical Innovations, LLC, shown in Figure 1(a). Since power settings and argon gas flow rates vary with the type of

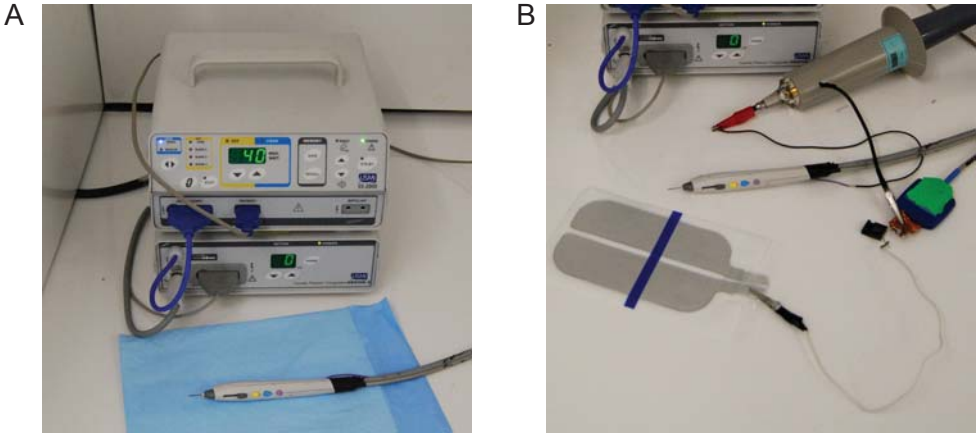


**FIG. 1:** (a) USMI Electrosurgical system SS-200E and the argon delivery unit Argon 2 coupled with the Canady Hybrid Plasma Scalpel from US Medical Innovations, LLC; (b) Experimental components: patient port from the ESU connected to a noninductive thin film resistor and USMI patient pad, high voltage probe, and USMI plasma scalpel.

treatment, we selected conditions representative of clinical uses. The SS-200E/Argon-2 was operated in coagulation mode at 40, 60, and 80 W with a 3 LPM flow rate of argon. The patient port of the ESU was grounded in all experiments. Several raw animal tissue samples were purchased frozen from a local food store and were thawed to 18–21°C before being used for the experiment. The scalpel was positioned between 2–6 mm away from the biological tissue for 2–5 sec to achieve stable and continuous flow of argon plasma. The depth of the burn injury was neither taken into account nor investigated in this study.

## A. Power and Tissue Resistance

The power produced by the ESU generator across the $R_L$ was measured. Various non-inductive thin film shunt resistors (0.2, 0.5, 1, 5, 10, 15, 20, 30, and 40 kΩ) were placed in series to determine the current produced by the circuit. The resistors were connected directly to the high voltage generator and the patient port of the ESU as shown in Figure 2(a). The voltage produced by the ESU was measured with the high voltage probe shown in Figure 1(b). The experiment was conducted at the power settings of 40, 60, and 80 W, and the actual power produced was calculated from

$$P = \left(\frac{U^2}{R}\right),$$

where U is the measured voltage produced by the scalpel and $R_L$ = 0.2, 0.5, 1, 5, 10, 15, 20, 30, and 40 kΩ.

The ranges of equivalent resistance for the biological samples during APC treatments were determined following observations from the first experiment. Samples containing different densities of muscle and connective tissue were selected. Raw animal tissue samples from pork belly, cow pectoral muscle, lamb liver, chicken liver, and chicken leg were tested as shown in Figure 2(b). A 10-Ω inductive thin film shunt resistor was used to determine the current generated in the circuit. The distance between the plasma scalpel and the tissue was measured and kept between 2 and 6 mm.

Additionally, the power distribution between plasma and tissue was investigated following the schematic shown in Figure 2(c). The replica, comprised of two metal electrodes separated by a deionized water gap, was used for testing (Fig. 3). Voltages were measured on both sides of the plasma channel, and the current was calculated using Ohm's law and a 10 Ω shunt resistor. Measurements between the tip of the plasma scalpel and the tip of the replica electrode were taken at 3, 4, 5, and 6 mm. The distances selected were within the acceptable range for maintaining a stable plasma flow. The power delivered to the plasma and tissue replica was determined by numerically integrating the instantaneous powers.

## B. Conductivity Measurements

A four-point probe method was used to determine the resistance of the fresh chicken samples. A set of voltage electrodes, spaced 1–2 cm apart, was placed in the sample between the two current electrodes. A 300 Ω shunt resistor was used to determine the

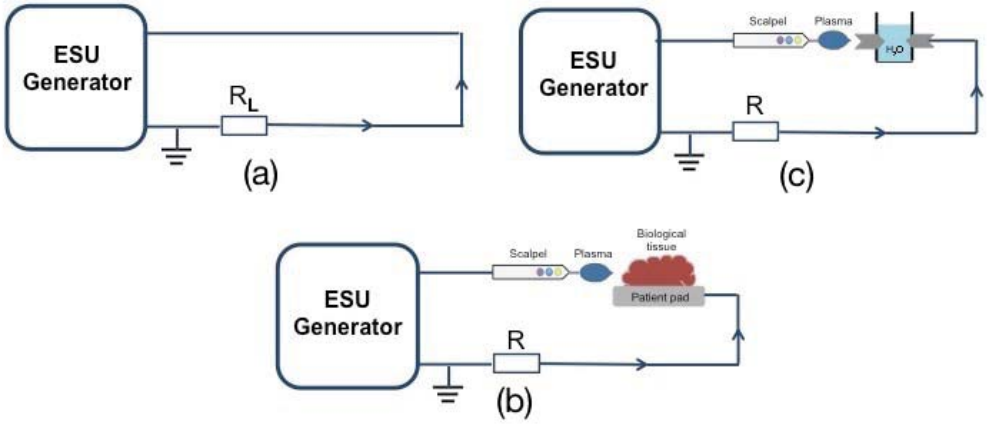


**FIG. 2:** Electrical schematics: (a) actual power produced by the ESU during coagulation across $R_L$ of 0.2, 0.5, 1, 5, 10, 15, 20, 30 and 40 kΩ, (b) equivalent tissue resistance experimental set-up, and (c) power distribution experiment with a deionized water sample as tissue replica

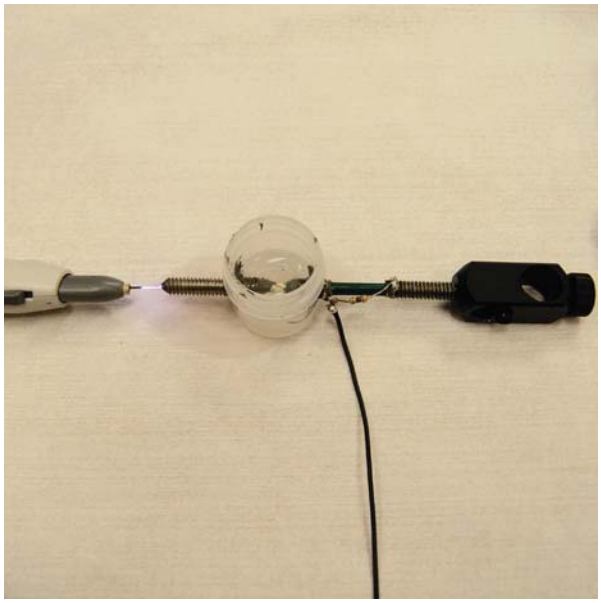

**FIG. 3:** Plasma scalpel directed at the tip of the tissue replica electrode.

current produced by the power source. The AC power source was set to 5 volts. The specific conductance between the inner electrodes was determined by measuring the current across the resistor as well as the voltage drop across the inner electrodes that were embedded in the sample. The two-point probe method was used to determine the relative conductivity between the surface of the untreated and treated tissue.

## III. RESULTS AND DISCUSSIONS

### A. Power Produced during Coagulation

Figure 4 compares the actual power produced by the ESU generator to the load resistance at the power settings of 40, 60, and 80 W. As the resistance approached 1 kΩ, the applied and set powers were similar. The actual power produced by the ESU generator ranged within 10%–15% from the power setting for all tested conditions. The gray bar in Figure 4 indicates this trend and shows that the resistance of the biological tissue is expected to be close to 1 kΩ during APC treatment. The data also revealed that the power decreased and neared zero when the $R_L$ was greater than 10 kΩ. Figure 4 reveals that for resistances greater than 1 kΩ, the instrument was able to produce power that was lower than that of the power setting. If the resistance of the tissue was substantially less than 1 kΩ, the applied power may lead to extensive tissue injury. The difference in power can be attributed to the resistance of the instrument because each power setting corresponds to an average resistance, which can be limiting. The user cannot modify this characteristic of the APC system, which could prove to be a major safety concern. The data suggested that the power setting could be adjusted based on the expected resistance of the tissue.

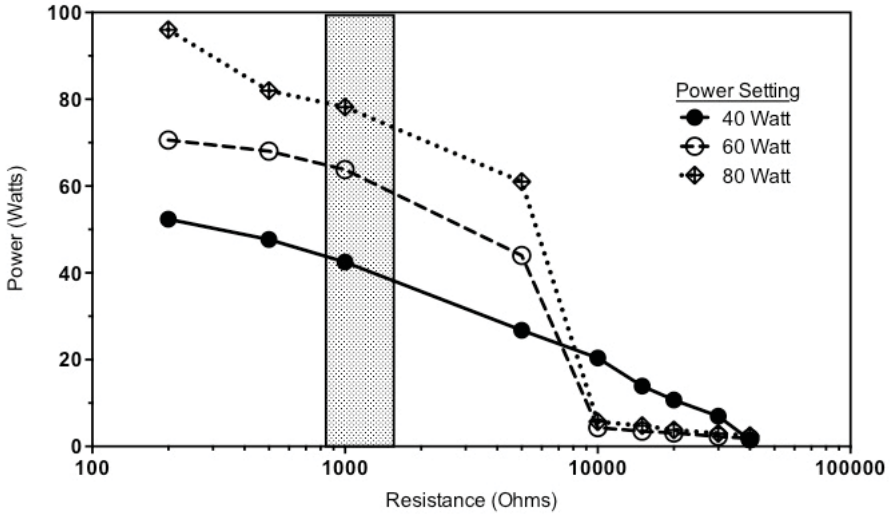


**FIG. 4:** Graph curve of the actual power produced by the ESU against the load resistance ($R_L$ of 0.2, 0.5, 1, 5, 10, 15, 20, 30, and 40 kΩ) for 40, 60, and 80 W of applied power.

### B. Equivalent Tissue Resistance and Conductivity

Figure 5 compares the resistance of five animal samples during APC treatment. The equivalent resistance for each biological sample was calculated by dividing the mea-

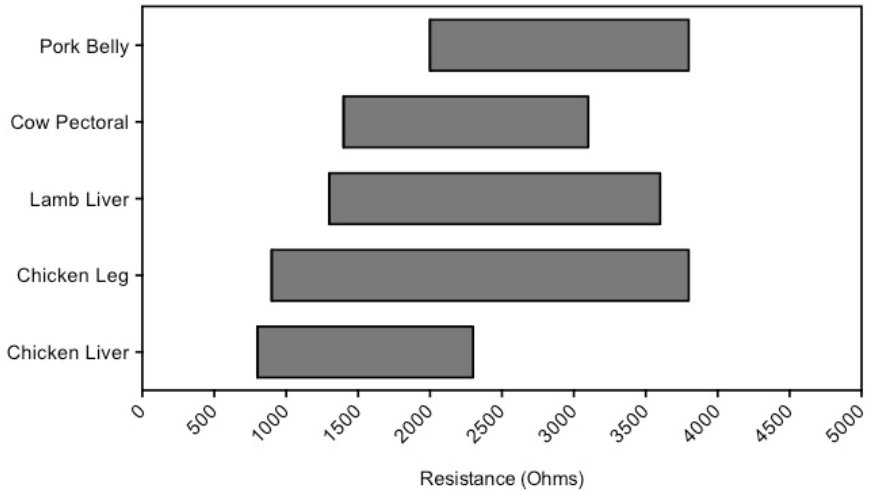


**FIG. 5:** Range of equivalent resistance for different types of animal tissue samples.

sured voltage by the discharge current for the time periods of the plasma discharge. The observed equivalent resistance ($R_{eq}$) ranged from 0.8 to 3.7 kΩ. We anticipated that human and animal tissue would have similar resistance ranges. To confirm these findings, the conductivity of animal tissue was measured and compared with the conductivity range previously reported for human tissue.

The reported conductivity for different human and animal tissues encompasses a large range (0.02–1.4 S/m), in part due to the different methods used for carrying out the measurements. For example, Bodakian and Hart[21] reported low values for the conductivity of chicken samples varying from 0.02 to 0.025 S/m, which may have resulted from using the two-point probe method.[21] With the four-point probe, we observed that the contact voltage drop at the probe-tissue interface was higher than the contact voltage drop of the tissue. The two-point method does not account for this voltage drop, therefore the literature reported values for conductivity might be underestimated.

The conductivity of our samples ranged from 0.2 to 0.6 S/m. Haemmerich et al.[18] reported the conductivity of liver tumor tissue to be 0.4–0.5 S/m. Our measured conductivity range was in accordance with the values reported in the literature for both healthy and tumor tissue.[18–27] Based on these findings we established that during APC treatment the resistance of human tissue is similar to that of animal tissue.

Figure 6 shows the surface of the chicken sample after treatment with argon plasma. The electrical conductivity of the cauterized samples was determined using relative measurements of the untreated and cauterized surfaces. We established a coefficient (α) to characterize the change in conductivity.

$$\alpha = \left( \frac{\sigma_c}{\sigma_{nc}} \right) \tag{1}$$

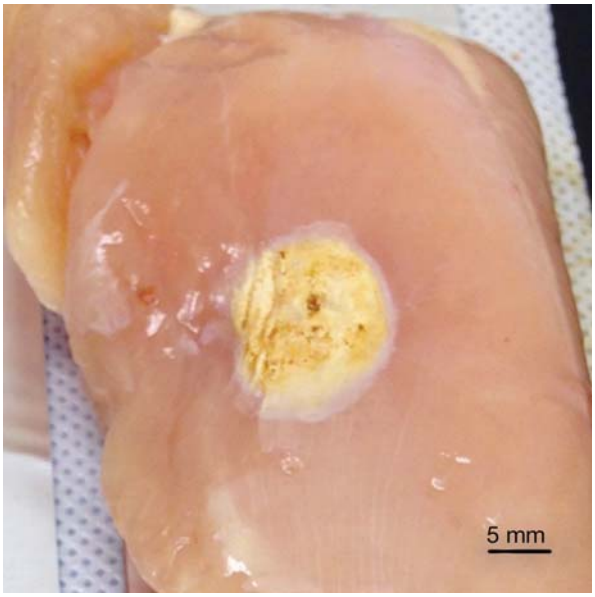


**FIG. 6:** The surface of a chicken sample after APC treatment. Scar diameter: 1 cm.

where $_c$ and $_{nc}$ are the conductivities in the cauterized area and noncauterized areas of the living tissue, respectively. The $\left(\frac{\sigma_c}{\sigma_{nc}}\right)$ ratio was determined using a current probe.

The probe, comprised of two conducting electrodes set 3 mm apart, provided stable contact with the tissue. The voltage difference between the probe wires was kept at 1 volt. Numerous current measurements were recorded to determine the average currents in the cauterized ($i_c$) and the noncauterized areas ($i_{nc}$). The $\alpha$ coefficient was determined as follows:

$$\alpha = \left(\frac{\sigma_c}{\sigma_{nc}}\right) = \left(\frac{i_c}{i_{nc}}\right) \tag{2}$$

The range for the $\alpha$ coefficient was calculated to be from 0.3 to 0.5, which indicated that the cauterized area had lower conductivity than the noncauterized one. This result was in support of the limited depth of injury that the APC treatment offers.

## C. Power Distribution

The power distribution between the tissue and plasma is shown in Figure 7. The experiment was conducted using a tissue replica, as shown in Figure 2(c). In a previous study, the waveforms of the discharge voltage and current generated for the chicken samples were compared with that of the deionized water replica. It was determined that their electrical discharges were similar[28] and therefore the replica was used for this testing. It was observed that 60%–80% of the power produced by the ESU was delivered to the tissue, whereas the rest was consumed for the production of the plasma. A portion of

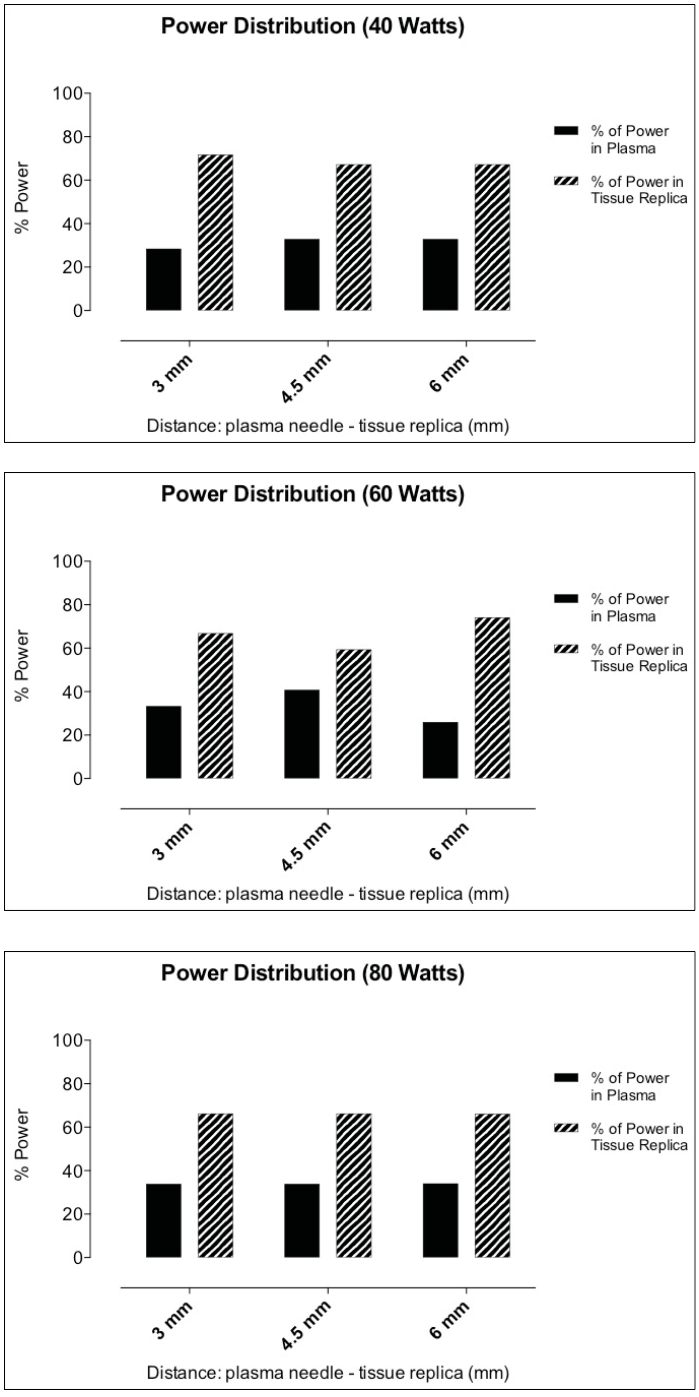


**FIG. 7:** Power distribution in plasma and tissue replica for power settings of (a) 40, (b) 60, (c) 80 W.

the power applied to the plasma channel was independent of the size of the gap created between the replica and the tip of the plasma scalpel in Figure 3. These findings are significant since, to our knowledge, there are no other studies that focused on the power distribution of APC systems during treatment.

## IV. CONCLUSION

Sample conductivity, resistance, and the amount of applied power determine the type of burn created by APC treatment. A burned surface caused from the brief exposure to argon plasma was determined to be two to three times less conductive than an untreated surface. The amount of power delivered to the treatment site was found to be dependent on the resistance of the tissue. If the resistance of the target tissue was outside the range of 0.8–3.7 kΩ, an inconsistent amount of power would be delivered, resulting in ineffective treatment. This study suggests that surgeons can adjust the power setting based on the expected resistance of the tissue being treated. When in the optimal resistance range, the majority of the applied power will be delivered to the target area, although a small percentage of it will be consumed by the plasma channel. Therefore, it is important to investigate APC units from different companies, because the accuracy of the delivered power may slightly differ among them. Inaccuracies in delivered power may greatly affect the treatment of many diseases.

## ACKNOWLEDGMENT

This research was supported by US Medical Innovations, LLC.

## REFERENCES

1. Norton ID, Wang L, Levine SA, Burgart LJ, Hofmeister EK, Yacavone RF. In vivo characterization of colonic thermal injury caused by argon plasma coagulation. Gastrointest Endosc. 2002;55:631–6.
2. Keidar M, Beilis II. Plasma engineering: applications from aerospace to bio and nanotechnology. Waltham, MA: Academic Press; 2013.
3. Canady J. Surgical Coagulation Device, US Patent, 1993/5207675.
4. Massarweh NN, Cosgriff N, Slakey DP. Electrosurgery: history, principles, and current and future uses. J Am Coll Surg. 2006;202:520–30.
5. Bolliger CT, Sutedja TG, Strausz J, Freitag L. Therapeutic bronchoscopy with immediate effect: laser, electrocautery, argon plasma coagulation and stents. Eur Respir J. 2006;27:1258–71.
6. Canady J, Wiley K, Ravo B. Argon plasma coagulation and the future applications for dual-mode endoscopic probes. Rev Gastroenterol Disord. 2006;6:1:1–12.
7. Laursen S, de Muckadell OS. Endoscopic management of nonvariceal upper gastrointestinal bleeding. Video J Encycl GI Endosc. 2013;1:122–4.
8. Malick KJ. Clinical applications of argon plasma coagulation in endoscopy. Gastroenterol Nurs. 2006;29:386–91
9. Kaassis M, Oberti F, Burtin P, Boye J. Argon plasma coagulation for the treatment of radiation proctitis. Endoscopy. 2000;32:673–6.
10. Grade AJ, Shah IA, Medlin SM, Ramirez FC. The efficacy and safety of argon plasma coagulation therapy in Barrett's esophagus. Gastrointest Endosc.1999;50:8–22.

11. Sagawa T, Takayama T, Oku T, Hayashi T, Ota H, Okamoto T, Muramatsu H, Katsuki S, Sato Y, Niitsu Y. Argon plasma coagulation for successful treatment of early gastric cancer with intramucosal invasion. Gut. 2003;52:334–9.
12. Byrne JP, Armstrong GR, Attwood SE. Restoration of the normal squamous lining in Barrett's esophagus by argon beam plasma coagulation. Am J Gastroenterol. 1998;93:1810–5.
13. Yusoff I, Brennan F, Ormonde D, Laurence B. Argon plasma coagulation for treatment of watermelon stomach. Endoscopy. 2002;34:407–10.
14. Canady J, Shashurin A, Wiley K, Fisch NJ, Keidar M. Characterization of plasma parameters and tissue injury produced by plasma electrosurgical systems. Plasma Med. 2013;3:279–89.
15. Goulet CJ, Disario JA, Emerson L, Hilden K, Holubkov R, Fang JC. In vivo evaluation of argon plasma coagulation in a porcine model. Gastrointest Endosc. 2007;65:457–62
16. Saul C, Toneloto EB, Rynkowski CB, Blaya C, Alegre P. High power setting argon plasma coagulation for the eradication of Barrett's esophagus. Am J Gastroenterol. 2000;95:1661–8.
17. Wahab PJ, Mulder CJJ, den Hartog G, Thies JE. Argon plasma coagulation in flexible gastrointestinal endoscopy: pilot experiences. Endoscopy. 1997;29:176–81.
18. Haemmerich D, Schutt DJ, Wright AW, Webster JG, Mahvi DM. Electrical conductivity measurement of excised human metastatic liver tumours before and after thermal ablation. Physiol Meas. 2009;30:5: 459–66.
19. Miklavčič, D, Pavšelj N, Hart FX. Electric properties of tissues. In: Wiley encyclopedia of biomedical engineering. 2006;209:1–12.
20. Burger HC, Dongen RV. Specific electric resistance of body tissues. Phys Med Biol. 1961;5:431–47.
21. Bodakian B, Hart FX. Dielectric properties of meat. IEEE Trans Dielectr Electr Insul. 1994;1:181–7.
22. Schwan HP, Kay CF. The conductivity of living tissues. Ann. N Y Acad Sci. 1957;65:1007–13.
23. Gabriel S, Lau RW, Gabriel C. The dielectric properties of biological tissues: II. Measurements in the frequency range 10 Hz to 20 GHz. Phys Med Biol. 1996;41:2251–69.
24. Gabriel C, Peyman A, Grant EH. Electrical conductivity of tissue at frequencies below 1 MHz. Phys Med Biol. 2009;54:4863–78.
25. Gabriel C, Gabriel S, Corthout E. The dielectric properties of biological tissues. 1. Literature survey. Phys Med Biol. 1996;41:2231–49.
26. Faes, TJC, Van der Meij HA, De Munck JC, Heethaar RM. The electric resistivity of human tissues (100 Hz-10 MHz): a meta-analysis of review studies. Physiological measurement, 1999; 20(4), R1.
27. Faes T, Meij H, Munck J, Heethaar R. The electric resistivity of human tissues (100 Hz-10 Mhz): a meta-analysis of review studies. Physiol Meas.1999;20(4):R1-10.
28. Shashurin A, Scott D, Zhuang T, Canady J, Beilis II, Keidar M. Electric discharge during electrosurgery. Sci Rep. 2015;5:9946.